Defense Technical Information Center
Compilation Part Notice

ADP013370

TITLE: Rapid Gel Cast Prototyping of Complex Paraelectric [Ba,Sr]TiO[3]/MgO Composites

DISTRIBUTION: Approved for public release, distribution unlimited

This paper is part of the following report:

TITLE: Materials Research Society Symposium Proceedings; Volume 720. Materials Issues for Tunable RF and Microwave Devices III Held in San Francisco, California on April 2-3, 2002

To order the complete compilation report, use: ADA410712

The component part is provided here to allow users access to individually authored sections of proceedings, annals, symposia, etc. However, the component should be considered within the context of the overall compilation report and not as a stand-alone technical report.

The following component part numbers comprise the compilation report:
ADP013342 thru ADP013370

Rapid Gel Cast Prototyping of Complex Paraelectric (Ba,Sr)TiO₃/MgO Composites

Jennifer Synowczynski, Samuel Hirsch, and Bonnie Gersten
Weapons and Materials Research Directorate, Army Research Laboratory
Aberdeen Proving Grounds, MD 21005-5069

ABSTRACT

A rapid prototyping process for manufacturing complex three-dimensional RF structures in ceramic systems was developed. The process combines fundamentals from lost wax investment casting and ceramic gelcasting. The first step is to directly deposit a mold made of a low melting point wax using a high precision inkjet rapid prototyper. Then, a gelcasting slurry containing polymeric precursors, a high solids loading of ceramic powders and a free radical initiator is cast into the mold and polymerized to lock in the structure. Finally, the mold is melted and the remaining green part is sintered. Aqueous gelcasting slurries were developed for $MgCO_3$, $(Ba,Sr)TiO_3$, and a composite of $(Ba,Sr)TiO_3$ and MgO. The maximum solids loading attained for each of the powders was 22 V%, 50 V%, and 25 V% respectively. The 50V% gelcast part had a more uniform microstructure, higher sintered density, less open porosity and smaller grain size than parts produced through dry pressing. The microstructural improvements resulted in a high dielectric permittivity.

INTRODUCTION

Recent efforts to reduce the weight, cost, and size of microwave devices such as electronic scanning antennas and voltage tunable filters have created the need for low-loss, voltage-tunable paraelectric materials. The critical materials parameters for RF device designs are (1) low dielectric constant for impedance matching (ε_R ~100) (2) low dielectric loss tangent (3) high tunability (i.e. % change in dielectric constant with voltage) and (4) small temperature coefficient of permittivity. To meet these requirements, investigators at ARL [1,2] composite paraelectric $(Ba,Sr)TiO_3$ (BST) with the low-loss, temperature-stable dielectric MgO. The resulting voltage-tunable materials have dielectric constants in the range from 800 to 100 and loss tangents as low as 0.008 at 10GHz with a voltage tunability of 7% at 2 volts/micron. New processing challenges arise for more complicated three-dimensional structures such as photonic bandgap devices [3]. In this investigation, we seek to develop a rapid prototyping method based on ceramic gelcasting and lost wax investment casting for manufacturing complex 3D structures from BST / MgO composites.

There are four major steps in lost wax investment casting: (1) create a sacrificial mold (2) cast a concentrated ceramic slurry into the mold (3) cure the slurry and (4) remove the mold. The ceramic slurry must have no destructive chemical interactions with the wax mold, a cure temperature below the mold softening point, and minimal drying shrinkage. Ideally, it would also produce a homogeneous microstructure and have a high green strength at low binder concentration. Of the available casting methods (slip casting, injection molding, physical gelation, etc [4, 5], chemical gelation (a.k.a gelcasting [6]) comes closest to meeting these requirements. Gelcasting forms a permanently bonded polymeric network with high green strength that locks the ceramic particles in place. This network also locks in an open pore structure making it easier to remove the solvent. Since the solids loading is high (>50V%), there is little drying shrinkage during solvent removal. Gelcasting can be used to make large (>6kg) or

small parts with submillimeter features and few defects. These advantages make it the ideal choice for a lost wax investment casting process.

EXPERIMENTAL DETAILS

Prototype Accuprop Mold

Disperse Powders in Premix at 20, 30, 40, 50 V%

Deair Slurry (15 min.)

Add Catalyst .01 g / g initiator

Room Temp. Cure (1 – 5 hr)

Vacuum Cast into Mold

Deair Slurry (5 min.)

Add Initiator 2, 4, 6 µl / g powder

Dry 3 hrs @ 50°C 95+% humidity

Melt Mold 130°C

Sinter Part 1350 – 1450°C
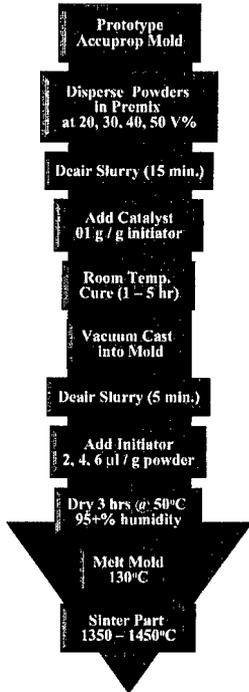
Figure 1. Process Flow Diagram

Figure 1 contains the process flow diagram and experimental conditions for the lost wax investment casting / ceramic gelcasting procedure. The accuprop molds were prototyped on our high precision Sanders Rapid Toolmaker in 0.05mm thick layers. All powders in the study were characterized to determine their surface area and particle size using BET (Micromeretics ASAP 2010) and dynamic laser scattering (Horiba LA-910). The dispersants listed in Table 1 were screened for their effect on the rheological properties (Brookfield Model LDTDV-I viscometer, small sample adapter, 20°C) of slurries containing a 20 V% loading of BST / MgO powders. The rheological properties of 35 V% BST slurries with DAR concentrations between 0 and 2 wt% were also measured. To determine the optimal initiator concentration, we conducted spectroscopic investigations (950 Raman Spectrometer, Nicolet Inst., WI) of the cure kinetics of the MAM-MBAM polymerization reaction. The polymeric distribution within the green bodies and the resulting sintered grain size distribution were monitored via Scanning Electron Microscopy (JEOL 840A, Japan). The Archimedes method was used to determine the open porosity and sintered density. Finally, low frequency dielectric properties were established through parallel plate capacitance measurements (HP4194 LCR) using Ag electrodes with a guard ring configuration.

Table I. Chemicals Investigated

Powder (Supplier)
BST - $Ba_{0.55}Sr_{0.45}TiO_3$ (see ref. 1)
BST / MgO – 40 wt% $Ba_{0.55}Sr_{0.45}TiO_3$ / 60 wt% MgO (see ref. 1)
$MgCO_3$ (Alfa Aesar, MA) + 3 wt% oxalic acid (Fisher Scientific, NY)
MgO (Alfa Aesar, MA)
Surfactant (Supplier) – 1wt% based on powder
DAR – Darvan 821A (RT Vanderbilt, CT)
PAA - Polyacrylic acid (Acros Organics, NJ)
HPC - Hydroxypropyl cellulose (m.w. 100,000 Alfa Aesar, MD)
DAXAD 32 - Ammonium polymethacrylate (WR Grace, KY)
DAXAD 34 - Polymethacrylic acid (Hampshire Chemical, MA),
EDTA - Ethylenediaminetetraacetic acid (Aldrich, WI)
SH - Sodium hexametaphosphate (Mallinckrodt, KY)
Aerosol 22 (Cytec, NJ)

Monomer and Crosslinker (Supplier)
MAM - methylacrylamide (98%, Aldrich, WI)
MBAM - methylene bisacrylamide (Aldrich, WI)
PEGDMA - poly(ethylene glycol) dimethacrylate (Aldrich, WI)
Premix (monomer:crosslinker, wt% in water)
MAM:MBAM (5:1, 12%)
MAM:PEGDMA (1:1, 15%)
Defoamer - 0.01 g/g powder (Supplier)
SURF - Surfnyol (Air Products and Chemicals, PA)
Catalyst - 0.01 g/g initiator (Supplier)
TEMED - tetramethylethylene diamene (Avocado Chemical, LS)
Free Radical Initiator - 2, 4, 6 μl / g powder (Supplier)
APS - ammonium persulfate (Aldrich, WI)

DISCUSSION

The surface area and median particle size were 1.639 ± 0.0175 m^2/g and 5.3μm for Ba $_{0.55}$Sr$_{0.45}$TiO$_3$ and 30.912 ± 0.1632 m^2/g and 5.2 μm for MgCO$_3$. The 40 wt% Ba $_{0.55}$Sr$_{0.45}$TiO$_3$/ 60wt% MgO powder had a bimodal distribution with a surface area of 4.751 ± 0.636 m^2/g and median particle sizes of 0.3μm and 1.2μm. Of the dispersants evaluated DAR, PAA, and SH yielded the least viscous slips (cf. Table II). Since SH contains inorganic contaminants that may adversely affect the dielectric properties, PAA and DAR were chosen for further optimization.

Table II. Effect of dispersants on room temperature viscosity

Dispersant ID	Viscosity (cp)
DAR	230
PAA	213
SH	264
EDTA	712
DAXAD 32	864
Aerosol 22	963
DAXAD 34	1124
HPC	5512

As shown in Figure 1a, the viscosity curve had a minimum at 0.085 wt% PAA, whereas DAR yielded fluid slips for all concentrations less than 1.75 wt%. The maximum castable BaSrTiO$_3$ loading was 35 V% for 0.125 wt% PAA [7] and 50V% for 1 wt% DAR. Slips made with 1 wt% DAR showed shear thinning behavior (cf. figure 1B). The degree of shear thinning and the viscosity increased as the solids loading increased. At loading > 40V%, the slips also exhibited slight thixotropic hysteresis. The change in viscoelastic properties at higher solids loading may be due to the short interparticle distance forming a particle network. This network breaks down at high shear rates (i.e. shear thinning) into individual flocs that flow past each other. As it breaks down the constrained solvent is freed, thereby reducing the effective volume fraction of the flocs and leading to thixotropic behavior.
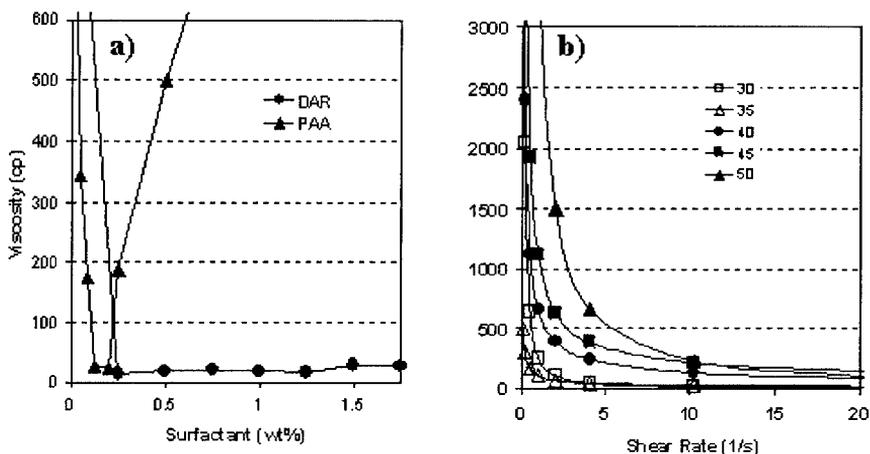
Figure 1. Viscosity vs. a) wt% surfactant b) shear rate (30, 35, 40, 45, 50 V%) with 1% DAR.

The MAM-MBAM curing kinetics were determined through the disappearance of the C=C bond at 1640 cm^{-1} and the emergence of the C-C at 1200 cm^{-1} (cf. Figure 2a). Results indicate that initiator concentrations less than 4 µl/g provided sufficient time to deair and cast the slurries. However, the kinetics change when BST is added to the gel. This change cannot be directly monitored using Raman spectroscopy because BST produces a strong fluorescence peak over a broad frequency range. This may be prevented in the future by changing the frequency of the laser.
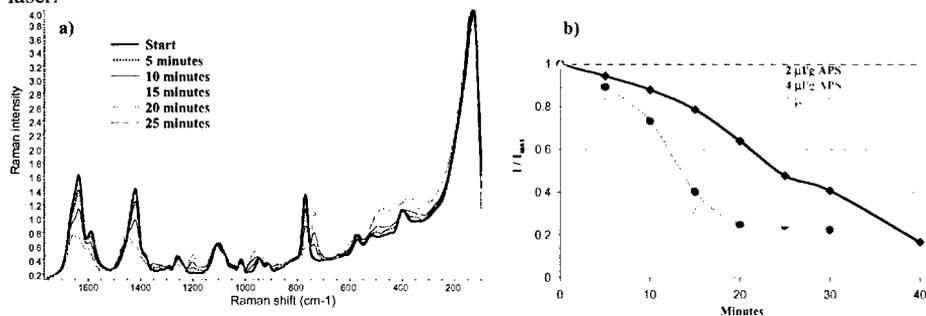
Figure 2. a) Cure Kinetics at 6µl/g initiator concentration b) 1640 band intensity vs. time.

Slurries containing 2µl/g initiator and 50V% $BaSrTiO_3$ were successfully cast and sintered (cf. Figure 4a). Parts cast under the same conditions but using the composite BST / MgO powders did not fully cure at room temperature after 24 hours. They lacked sufficient green strength to survive the dewaxing procedure. SEM analysis of the green bodies (cf. Figure 3a) revealed that the polymer network consisted of short chains that may have prematurely polymerized due to the interaction of dissolved Mg with the functional group of the monomer. To prevent this interaction, the solubility of Mg in water was reduced by switching to $MgCO_3$

and coating the particles with oxalic acid to produce a thin surface layer of magnesium oxalate (cf. Figure 3b).
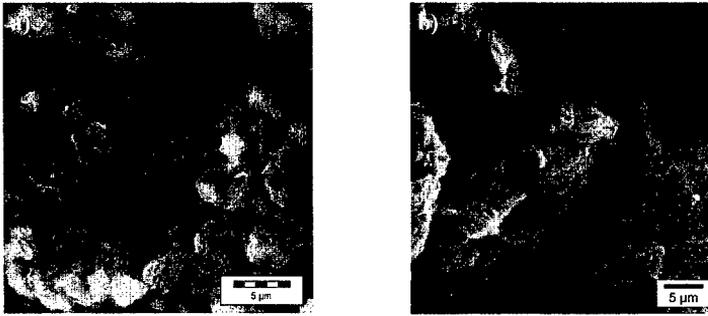
Figure 3. Green body interior a) 40wt% Ba $_{0.55}$Sr$_{0.45}$TiO$_3$/ 60wt% MgO b) coated MgCO$_3$.

Table III lists the microstructural analysis and dielectric properties for the sintered composites. For BST, the green and sintered densities did not change significantly as the solids loading increased from 30 to 45 V%. However, at 50 V% they exceeded the properties attained through dry pressing. The grain size was consistently lower for gelcast samples than the dry pressed. The combination of higher density and smaller grain size lead to improvements in the permittivity and dielectric loss tangent. For the composite gelcasts, the sintered density increased as the solids loading increased. The solids loading attained was not high enough for the density to equal that obtained during dry pressing. This degraded the electrical performance. However, the BST and MgO grains were more uniformly distributed in the gelcast samples (cf. Figure 4b,c). The segregation in the dry pressed samples is most likely due to agglomeration and differential settling within the die set caused by differences in the density and particle size of the powders. Since gelcasting is a colloidal process, the powders are uniformly dispersed immediately prior to producing the green body.

Table III. Microstructural and Dielectric Properties.

MgO (wt%)	Solids (V%)	Green ρ (g/cc)	Sinter ρ (g/cc)	% Open Porosity	Grain Area (μm^2)	ε_R (1MHz)	Tanδ (1MHz)
0	Pressed	2.53	5.05	3.1	74 ± 34	2597	0.0010
0	25	2.21	4.89	6.5	44 ± 23	2065	0.0013
0	30	2.37	5.20	4.6	150 ± 136	2360	0.0010
0	35	2.51	5.20	6.2	52 ± 38	2360	0.0009
0	40	2.44	5.17	1.9	49 ± 33	2331	0.0014
0	45	2.44	5.16	0.6	50 ± 22	2150	0.0010
0	50	2.66	5.40	2.6	56 ± 28	2651	0.0006
60	Pressed	2.23	4.30	3.1		81	0.0002
60	15	1.24	2.84			45	0.0010
60	20	1.51	3.23	3.2		68	0.0002
60	25	1.34	3.80	1.9		74	0.0004
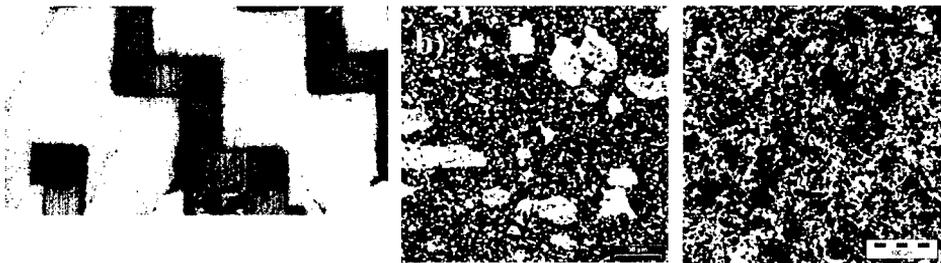
Figure 4. Microstructure of 40wt% Ba$_{0.45}$Sr$_{0.55}$TiO$_3$/ 60wt% MgO a) dry pressed b) gelcast.

CONCLUSION

Three-dimensional paraelectric parts were cast using a combination of lost wax investment casting and ceramic gelcasting. The most fluid slips were prepared using darvan 821A at concentrations less than 1.75 wt% based on powder. These slurries were shear thinning and slightly thixotropic at high solid loading. The maximum loading attained was 50V%, 22V%, and 25V% for Ba$_{0.55}$Sr$_{0.45}$TiO$_3$, MgCO$_3$, and 40wt% Ba$_{0.45}$Sr$_{0.55}$TiO$_3$ / 60wt% MgO respectively. The BaSrTiO$_3$ gelcast samples had a smaller grain size, more uniform microstructure and higher sintered density than the dry pressed. This resulted in improvements in the low frequency permittivity and dielectric loss tangent over the conventionally processed Ba$_{0.55}$Sr$_{0.45}$TiO$_3$. It was not possible to achieve the same solids loading for aqueous MgO slurries due to their unique surface chemistry. Lower loadings resulted in low-density parts with poor dielectric properties. By coating the particle surface with magnesium oxalate, the interaction between the dissolved Mg and the functional group of the monomer was eliminated. In the future, the solids loading may be improved by either switching to a non-aqueous gelcasting system or coating the MgO surface to change the surface chemistry.

ACKNOWLEDGEMENTS

REFERENCES

1. J. Synowczynski, B. Gersten, Army Science Conference, December (2000).
2. J. Synowczynski, L. Sengupta and L. Chiu, Integrated Ferroelectrics **22**[1-4] 861-872 (1998).
3. V. Berger, Optical Materials **11** 131-142 (1999).
4. W. Sigmund, J. Am. Ceram. Soc. **83**[7] 1557-74 (2000).
5. J. Lewis, J. Am. Ceram. Soc. **83**[10] 2341-59 (2000).
6. O. Omatete, M. Janney and S. Nunn, J. Euro. Ceram. Soc. **17**[2-3], 407-413 (1997).
7. J. Synowczynski, S. Hirsch, B. Gersten, Electroactive Polymers and Rapid Prototyping, MRS Fall Proceedings **698** in press (2001)